An ALS Therapeutic Assembly Modulator Target in Peripheral Blood Mononuclear Cells: Implications for ALS Pathophysiology, Therapeutics, and Diagnostics

Shao Feng Yu[1], Maya Michon[1], Anuradha F. Lingappa[1], Kumar Paulvannan[1], Dennis Solas[1], Kim Staats[2], Justin Ichida[2], Debendranath Dey[1], Jeffrey Rosenfeld[3] and Vishwanath R. Lingappa[1,4,5]

[1] Prosetta Biosciences, Inc. 670 5th St San Francisco, CA 94107

[2] University of Southern California, Los Angeles, CA 90033

[3] Loma Linda Medical Center, Loma Linda, CA 92354

[4] Department of Physiology, University of California, San Francisco, CA 94143

[5] To whom correspondence should be directed (vlingappa@prosetta.com)

Abstract

Assembly modulators are a new class of allosteric site-targeted therapeutic small molecules, some of which are effective at restoring nuclear localization of TDP-43 in ALS cellular models, and display efficacy in a variety of ALS animal models. One of these compounds has been shown to target a small subfraction of protein disulfide isomerase, a known allosteric modulator implicated in ALS pathophysiology, within a novel, transient, and energy-dependent multi-protein complex that includes other important members of the ALS interactome, such as TDP-43, RanGTPase, and selective autophagy receptor p62/SQSTM1. Building on earlier literature suggesting PBMC dysfunction in ALS, we demonstrate here that a similar multi-protein complex drug target is present in PBMCs with signature alterations in PBMCs from ALS patients compared to PBMCs from healthy individuals. ALS-associated changes in the drug target include increased RanGTPase and MMP9, diminished p62/SQSTM1, and most distinctively, appearance of a 17kDa post-translationally modified form of RanGTPase. Many of these changes are not readily apparent from analysis of whole cell extracts, as a number of the proteins present in the target multi-protein complex, including RanGTPase, comprise a miniscule percent of their total in cell extracts. A small subset of each of these proteins appear to come together in a transient, energy-dependent fashion, to form the drug target. Furthermore, whole blood from ALS patients shows a distinctive degradation of RanGTPase not observed in blood from healthy individuals, which appears to be rescued by treatment with either of two structurally unrelated ALS-active assembly modulators. Our findings are consistent with the hypothesis that ALS is fundamentally a disorder of homeostasis that can be both detected and treated by assembly modulators.

45 **Introduction**

46 Amyotrophic Lateral Sclerosis (ALS) is a devastating neurodegenerative disease that
47 strikes approximately 6,000 American and 150,000 people worldwide annually[1,2]. Approximately
48 10% of ALS is familial, with a large number of specific gene mutations implicated. The vast
49 majority of ALS cases however, are sporadic, meaning that that there is no family history of the
50 disease and therefore is likely due to an environmental or epigenetic influence. Specific
51 environmental factors have been implicated in causing ALS, but remain controversial and
52 inconclusive. While the pathophysiology is not well understood, aggregates of the protein TDP-
53 43 are almost invariably found in the brains of patients with ALS and fronto-temporal dementia
54 (FTD)[3]. This observation and the discovery of shared genetic mutation (C9orf72) suggest that
55 these diseases are therefore on a continuum of the same underlying disorder. Despite these
56 commonalities, the clinical presentation as well as progression of ALS, is highly variable[4].
57

58 With regards to TDP-43 pathophysiology, controversy exists as to the triggering event.
59 Some studies have implicated mislocalization of TDP-43 from the nucleus in healthy cells to the
60 cytoplasm, which is observed to variable degrees in fibroblasts from many, but not all, cases of
61 ALS[5]. An alternative view is that, in response to stress, TDP-43 forms aggregates in the
62 cytoplasm where it is synthesized, prior to transport to the nucleus[6]. A further controversy
63 exists as to whether the relevant TDP-43 aggregates in the cytoplasm are within, or outside of,
64 stress granules[7]. While the TDP-43 aggregates have generally been viewed as a trigger of motor
65 neuron death, it is possible that they are an epiphenomenon whose elimination *per se* may not
66 necessarily be therapeutic, by analogy to the failed attempts to remedy Alzheimer's Disease by

67 elimination of its pathognomonic Aβ aggregates. Regardless of their natural history and role in
68 the pathophysiology of ALS, the presence of TDP-43 aggregates are pathognomonic for the
69 disease[8,9].
70
71 Recently we presented our studies on the role of a newly appreciated dimension of gene
72 expression, termed protein assembly, in pathophysiology of diverse diseases, including ALS[10].
73 We have identified several structurally unrelated small molecule chemotypes termed assembly
74 modulators, that are strikingly efficacious, including at both preventing neurodegeneration and
75 correcting TDP-43 pathology, in various cellular and animal models of ALS[10]. The compounds are
76 broadly efficacious at reversing both TDP-43 mislocalization and stress-induced TDP-43
77 aggregation, in both familial and sporadic ALS cellular models[10]. Efficacy was also demonstrated
78 in various transgenic animals expressing human ALS-causing mutations including in TDP-43, FUS,
79 c9orf72, and SOD1[10]. In view of this breadth of efficacy, we hypothesized the mechanism of
80 action of the assembly modulator drug to target a step common to most, if not all, ALS. Analogs
81 of some of these compounds are close to completion of a target product profile for initiation of
82 investigational new drug (IND)-enabling studies in anticipation of human clinical trials in the
83 near future.
84
85 The studies to be described here had several motivations. First, to explore the
86 hypothesis that even physiological pathways thought of as well understood may have additional
87 layers of regulation yet to be discovered, in which the small molecule assembly modulators and
88 their novel multi-protein complex targets we have discovered, might be involved. How those

levels of control are integrated with one another and communicated from one organ system to others remains mysterious, for which the novel assembly modulator targets we have discovered are potential candidates. By corollary, what happens to other feedback controls when one level of regulation fails, remains to be determined. The argument has been made based on gene knockout experiments that back up pathway may be activated when primary regulatory controls fail[11]. Having a drug that impinges on a biochemical pathway in a novel way is a powerful means of probing biological regulation, particularly that which depends on information that does not reside simply in the sequence of the genome[12,13,14]. Thus the relevance of the compounds we have described, with their novel mechanism of action at allosteric sites[15,16], and the unconventional nature of the targeted multi-protein complex (energy-dependent for formation, transient in existence, composed of miniscule subsets of the individual component proteins in the cell)[17,18]. These tools may provide a new understanding of the molecular basis for homeostasis.

A second motivation for the present studies was to understand the meaning of the observed dysfunction of PBMCs in ALS[19,20]. These findings can be interpreted in two generally different ways. On the one hand, PBMC dysfunction might be due to ALS being a systemic disease whose most severe manifestation is motor neuron death, but which also manifests in less dramatic fashion in other organ systems, including in blood. Alternatively, dysfunction of PBMCs might be a consequence of disordered communication between organ systems, or its regulation. Thus, a disorder affecting one organ system could have a “domino effect” manifest in other organ systems. Even if ALS is initiated in motor neurons, their dysfunction may be

111 transmitted to other organ systems as a secondary consequence of feedback regulation
112 intended to maintain homeostasis. In either framework, or hybrids of the two, disordered
113 homeostasis is a fundamental feature of ALS pathophysiology. If a means of restoring
114 homeostasis could be identified it may be effective in therapeutics of many diseases including
115 ALS. Towards this end, we asked whether assembly modulator drugs, that are therapeutic in cell
116 and animal models for ALS, might also detect a disordered drug target in PBMCs from ALS
117 patients. If so, how does that target compare to the target observed in brain or patient-derived
118 fibroblasts (PDFs) in which TDP-43 pathology is observed?
119
120 Finally, apart from intellectually interesting questions of feedback and mechanism of
121 action, there is the practical desire to advance these compounds with remarkable therapeutic
122 properties in cellular and animal models, to the clinic. Having a readily accessible signature in
123 PBMCs could facilitate drug advancement in innumerable ways including for early detection of
124 ALS (prior to severe disability), patient enrollment and tracking response to therapy. Most
125 importantly, it could allow detection of ALS early when compounds that restore homeostasis
126 should be most effective.
127
128 **Results**
129 Blinded blood samples were obtained from ALS patients under an IRB-approved
130 protocol, PBMCs isolated, extracts prepared as described in methods, and analyzed for key
131 proteins relevant to ALS. No clear and consistent different was observed in the protein pattern

132 between PBMCs of healthy and ALS patients by total protein silver stain (see for example, **Figure**

133 **1A**).

134

135 However when PBMC extracts were applied to the ALS-active drug resin described

136 previously[10] versus control resin (lacking the drug ligand), washed and bound material analyzed,

137 a distinctive subset of proteins was observed, also largely shared between healthy individuals

138 and ALS patients, but with a few possible differences (black arrows in **Figure 1B**).

139

Figure 1

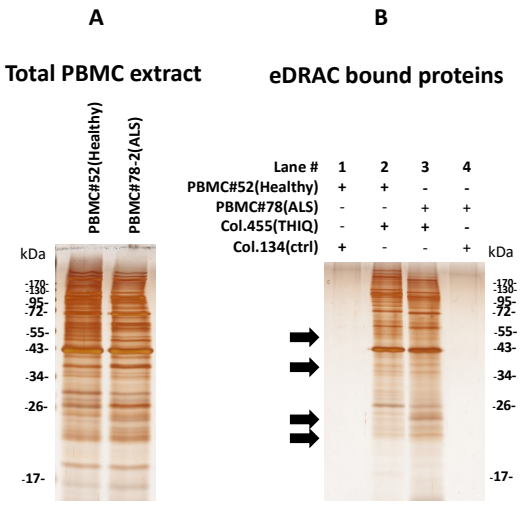

140

141 Legend to Figure 1. A. Silver stain of starting PBMC extract 10kxg/10min supernatant from a representative healthy

142 individual (#52) and an ALS patient (#78-2). B. Silver stain of free drug eluate from ALS-active assembly modulator

143 drug resin (column 455 THIQ) or control resin (column 134 lacking the drug ligand). Black arrows indicate positions

144 at which healthy vs ALS patient samples show a suggestive difference in the free drug eluate protein pattern.

145

146 Mass spectrometry analysis of free drug eluates from PBMCs applied to the ALS-active drug

147 resin (**Figure 2**) was carried out and compared to the pattern previous revealed from mouse

148 brain. A substantial proportion of tissue-specific proteins (~1/2 to 2/3 depending on the specific
149 sample) were observed (see Supplemental Figure 1). Despite the high tissue specificity, a core
150 set of 27 proteins were identified as shared between both PBMCs and brain, that are in the ALS
151 interactome. Notably, this set included P4HB, a member of the PDI family, two known ALS-
152 causing proteins (TUBA4A and VCP)[21], along with five proteins implicated in the KEGG ALS
153 interactome[22] (ATP5A1, HSPA5, TUBA1A, TUBA4A, and VCP). Furthermore, 24 of these 33
154 proteins exhibited high-confidence interactions with known ALS-causing or disease-modifying
155 proteins[21]. The 27 shared ALS interactome proteins also included multiple members of several
156 protein families and complexes: two ATP synthase subunits (ATP5A1 and ATP6V1A), six
157 chaperonins containing T-complex components (CCT2, CCT3, CCT4, CCT5, CCT7, and CCT8),
158 three thioredoxin domain proteins (P4HB, PRDX1, and PRDX2), and four members of the 14-3-3
159 family (YWHAB, YWHAE, YWHAH, and YWHAQ) (**Figure 2A**).
160
161 MCL clustering analysis was performed on the 33 shared proteins using the STRING
162 database, which integrates information from various databases cataloging known and predicted
163 protein-protein interactions. The analysis generated groups called "clusters," characterized by a
164 higher density of predicted associations within the clusters compared to those between
165 clusters. Notably, 31 out of the 33 proteins formed a single, highly interconnected cluster,
166 suggesting potential functional relationships between them. Two proteins, VAT1 and ALDH1A1,
167 were excluded from this cluster, as there are no predicted interactions between these proteins
168 and the other 31 proteins (**Figure 2B**).

Figure 2

A

	WT mouse THIQ eluate	WT mouse Control eluate	SOD mouse THIQ eluate	SOD mouse control eluate	Healthy PBMC 44 THIQ eluate	Healthy PBMC 52 THIQ eluate	ALS PBMC 43 THIQ eluate	ALS PBMC 53 THIQ eluate	ALS PBMC 43 Control eluate	Causitive genes	Associated and disease modifier genes	ALS protein binding partners	KEGG ALS interactome
ACTN4	7	0	4	0	64	69	78	69	0				
ALDH1A1	2	0	7	0	8	0	0	2	0				
ATP5A1	22	0	17	0	2	5	5	6	0				
ATP6V1A	13	0	7	0	3	0	5	0	0				
CALM1	11	0	10	0	13	13	11	12	0				
CCT2	8	0	13	0	7	0	3	0	0				
CCT3	6	0	2	0	8	2	6	2	0				
CCT4	3	0	6	0	8	0	3	2	0				
CCT5	9	0	8	0	9	2	5	0	0				
CCT7	4	0	6	0	8	0	4	0	0				
CCT8	8	0	7	0	11	0	7	2	0				
EEF1G	9	2	10	0	4	4	5	2	0				
HSP90AA1	37	0	44	0	20	13	15	11	0				
HSP90AB1	39	0	46	0	19	15	15	8	0				
HSPA5	11	0	15	0	0	7	0	0	0				
HSPB1	4	0	6	0	4	17	10	0	0				
HSPD1	38	2	38	0	12	21	12	9	0				
LDHB	7	0	0	0	14	0	12	0	0				
P4HB	16	0	23	0	54	48	64	43	0				
PRDX1	8	0	11	0	8	6	4	4	0				
PRDX2	7	0	10	0	18	8	9	19	0				
ST13	6	0	11	0	3	0	4	5	0				
STIP1	32	0	35	0	3	9	0	0	0				
TCP1	6	0	5	0	6	0	4	0	0				
TUBA1A	17	0	15	0	10	12	15	18	0				
TUBA4A	16	3	12	0	11	14	18	18	0				
USP5	12	0	23	0	5	0	2	0	0				
VAT1	9	0	10	0	4	0	10	3	0				
VCP	47	2	53	0	55	62	58	55	0				
YWHAB	9	0	0	0	12	6	9	0	0				
YWHAE	9	0	11	0	6	6	6	0	0				
YWHAH	6	0	7	0	6	7	8	0	0				
YWHAQ	10	0	9	0	0	5	6	7	0				

B

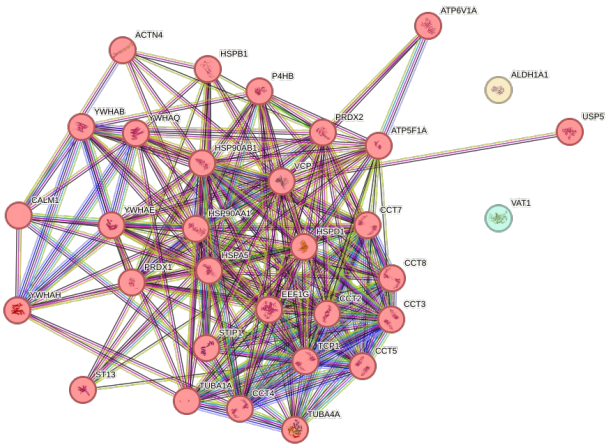

Legend to Figure 2. A**.** Spectral counts for proteins identified in THIQ drug resin eluate from mouse brain and human PBMC extracts. Colors represent the number of spectral counts for a given protein in each sample, ranging from light green (low counts) to dark green (high counts). The right panel indicates "hits" for proteins present in the ALS interactome, where yellow is a hit. B. STRING database protein-protein interaction network with MCL clustering. Each circle ("node") represents a protein, and each line ("edge") represents a predicted interaction between two nodes. Different colors represent distinct clusters identified by the MCL algorithm, with red indicating the largest cluster and yellow and green representing clusters containing only a single protein.

From the MS-MS analysis it was clear that the multi-protein complex isolated from PBMCs on the ALS-active drug resin appears related to that observed in mouse brain, based on the 27 shared proteins identified that are in the ALS protein interactome observed from both sources. However no clear differences between healthy and ALS patients were observed by MS-MS.

184

185 Recognizing that MS-MS can fail to identify specific proteins for a number of reasons,
186 including post-translational modification and failure of peptide ionization, we analyzed the
187 samples by western blot for particular proteins of interest including for TDP-43, RanGTPase, and
188 P62/SQSTM1 (Figure 3). By Western blotting a number of differences in proteins bound to the
189 assembly modulator THIQ drug resin were observed between healthy individuals and ALS
190 patient PBMC extracts. Most notably p62/SQSTM1 was greatly diminished and a 17kDa post-
191 translationally modified (PTM) fragment of RanGTPase detected in ALS patients compared to
192 healthy individuals.

Figure 3.

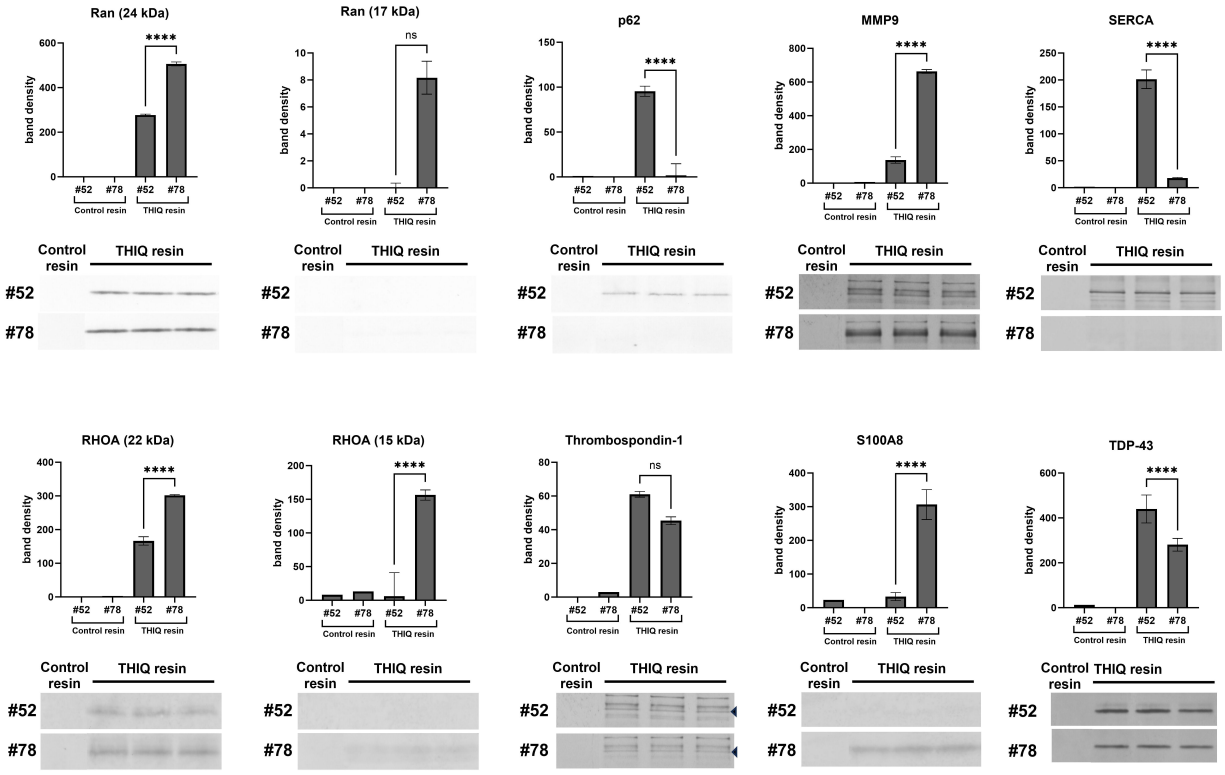

193

194 Legend to Figure 3. PBMC extracts were prepared as described in methods and applied to drug resin versus control
195 resin, washed and bound proteins analyzed by SDS-PAGE transferred to 0.2u PVDF membrane and Western blotted
196 for the indicated proteins with quantitation of bands using Image J software.
197

198 Next, photocrosslinking was carried out with PBMC extracts to which was added a drug
199 analog in which the attachment to resin was replaced with a biotin and diazirine moiety such
200 that exposure to UV light results in a covalent linkage to the drug binding protein(s). Under
201 native conditions associated proteins can be precipitated with streptavidin beads. If the sample
202 is first denatured, then only the direct drug-binding protein will be precipitated with
203 streptavidin beads under the conditions described. Figure 4 demonstrates that PDI is the direct
204 drug-binding protein. The PBMC extracts displayed striking similarities with the corresponding
205 drug resin complexes from brain. In particular, the direct drug-binding protein in extracts from
206 all three tissue sources, was PDI (Figure 4).
207

Figure 4.

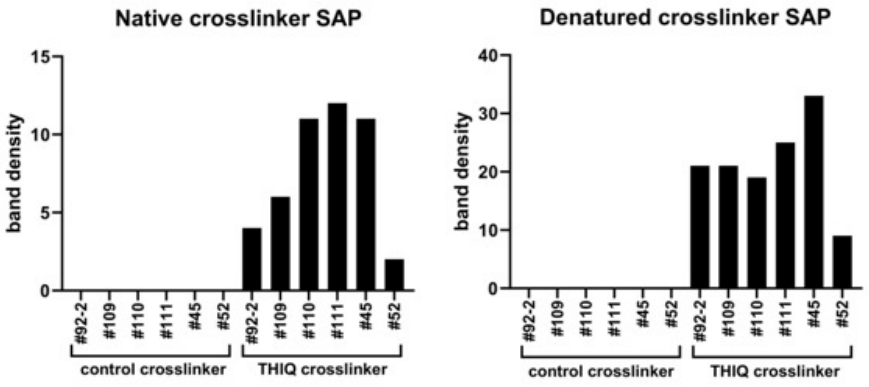

208

209 Legend to Figure 4. Quantitation of PDI in streptavidin precipitates under native vs denatured
210 conditions after photocrosslinking with PAV-073 analog (THIQ) or control crosslinker lacking the

211 drug ligand. Both control and THIQ crosslinkers contain biotin and diazirine as described in

212 methods and previously[10].

213

214 We then assessed whether the ALS patient vs healthy control correlations were temporal

215 in nature. As can be seen in Figure 5, with progression of disease, the amount of p62 bound to

216 the resin diminishes and intensity of the RanGTPase 17kDa fragment increases, with disease

217 progression. Notably, the diagnosis of ALS was made in pt 78 very early in her disease

218 progression. She was able to drive herself to the clinic and walk in with a cane, at the time that

219 the initial blood sample was taken.

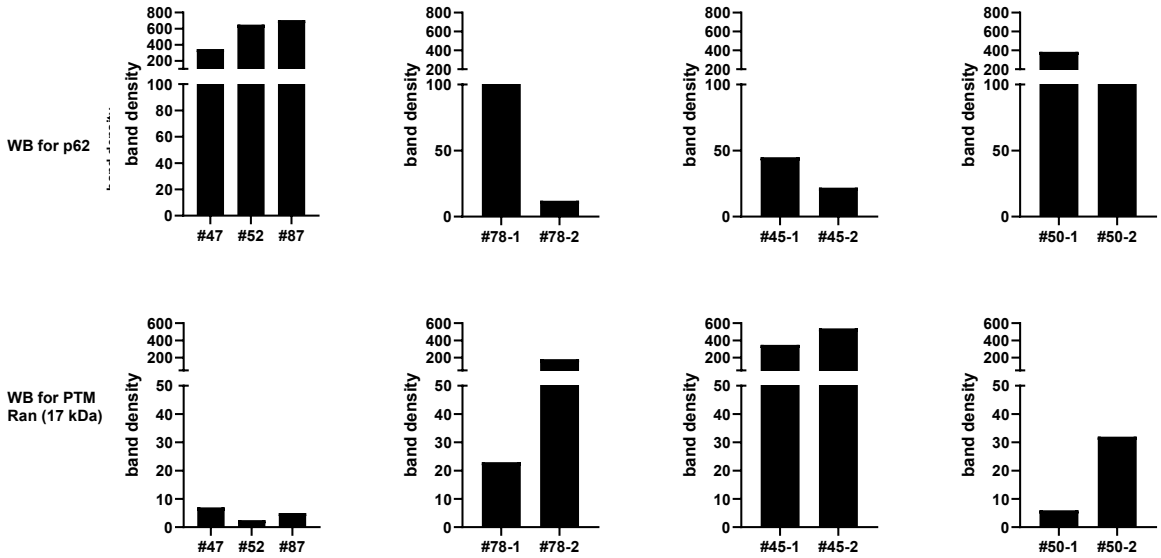

220

221 Legend to Figure 5. PBMC extracts were prepared as previously, applied to drug resins and bound proteins analyzed

222 by Western blotting for specific proteins of interest. Bands corresponding to the correct molecular weights were

223 quantified. The presence of an ALS-specific marker at an anomalous migration (17kDa) suggested the presence of a

224 post-translational modification.

225

226 Out of 16 ALS patients and 5 healthy controls assessed in a blinded fashion, 11 ALS patients and
227 0 healthy controls have the ALS-associated PBMC eDRAC eluate signatures noted, namely, loss
228 of p62/SQSTM1 and appearance of the 17kDA RanGTPase fragment. Thus, taken together, the
229 three eDRAC signatures observed appear to have a sensitivity exceeding 90% and a specificity
230 approaching 100%, albeit from a modest sample size.
231
232 If, as we suggest, ALS represents a breakdown in homeostasis where protective mechanisms to
233 reboot a cellular operating system are ineffective, certain predictions follow. For one, there may
234 be a back up mechanism activated in an attempt to correct the failure of the first line of
235 defense, although by definition in the subset of patients with ALS, that backup has failed to
236 correct the problem. In view of the distinctive ALS-associated appearance of a 17kDa
237 RanGTPase fragment as noted in Figure 5 above, degradation of RanGTPase, allowing its
238 resynthesis seemed like a plausible feedback response that could be readily assessed. A second
239 prediction is that if, as we hypothesize, assembly modulation is a fundamental mechanism of
240 regulation of gene expression and its activation by these compounds is therapeutic for ALS,
241 treatment of blood from ALS patients with the drugs should result in cessation of the back up
242 RanGTPase degradation feedback loop, upon restoration of the primary mechanism of
243 homeostatic control.
244
245 To test these hypotheses, we took blinded blood samples from ALS patients and healthy
246 controls and treated whole blood with two different, structurally unrelated assembly modulator
247 compounds versus vehicle control, and assess the impact after 72hrs of incubation (Figure 6). In

248 the healthy controls RanGTPase was observed to be stable. However in blood from ALS patients,

249 there were greatly diminished levels of RanGTPase after a brief incubation, consistent with what

250 would be expected for feedback degradation of dysfunctional RanGTPase (Figure 6A).

251 Upon treatment with either of two ALS assembly modulators for 72hrs, a striking restoration of

252 RanGTPase stability was observed, with no change in the level observed in healthy subjects.

Figure 6.

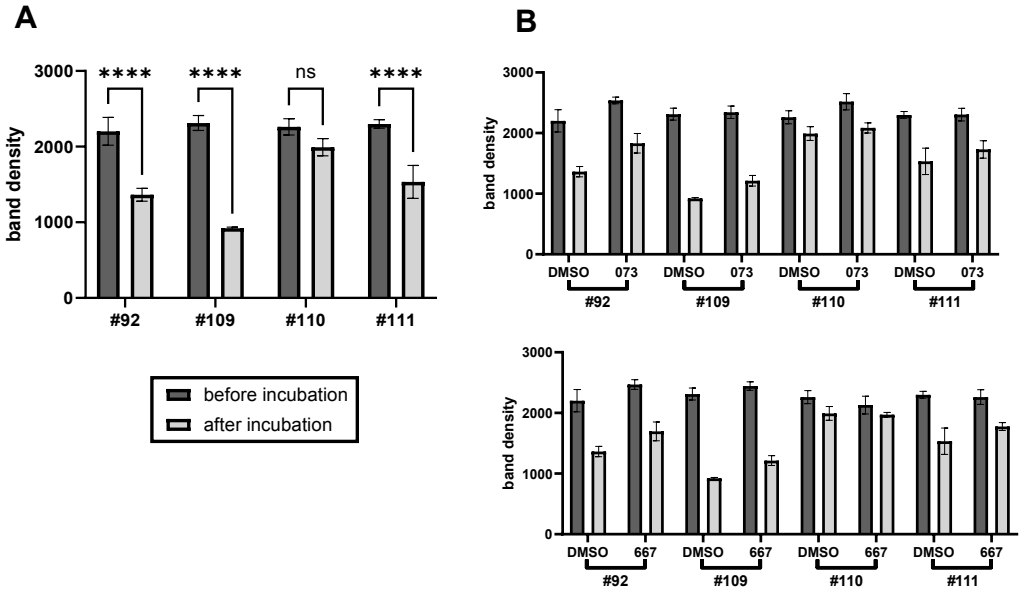

253

C

Chemotype	Molecular weight (g/mol)	log P	H-bond donors	H-bond acceptors	Topological polar surface area (Å²)	Tanimoto similarity coefficient
T	443.543	4.8	1	5	49	<20%
Q	441.915	6.4	0	7	73.7	<20%

254

255 Legend to Figure 6. A. 10mls of whole blood from ALS patients or healthy controls was collected under an IRB-approved protocol and shipped overnight at room temperature in EDTA-anticoagulated (purple top) tubes without any patient-specific confidential information. An aliquot of whole blood was taken, incubated in 1% SDS for one hour at 37°C, prepared for SDS-

256 PAGE, and set aside. Another aliquot of whole blood was mixed 1:1 with glucose-supplemented MEM and incubated for 72hrs at 37oC in the presence of vehicle, at the end of which it was processed as previously described, and analyzed by SDS-

257 PAGE. (-) refers to the sample prepared for SDS-PAGE immediately, while (+) refers to the sample incubated prior to preparation for SDS-PAGE. B. Samples of whole blood incubated for 72hr with two different assembly modulator drug chemotypes (called T and Q) or vehicle (D) were incubated for 1hr at 37oC in 1% SDS and then analyzed by SDS-PAGE and WB for RanGTPase. C. The two assembly modulator chemotypes studied in B. are compared for drug-like properties and Tanimoto similarity coefficient compared to one another.

258 **Discussion**

259 The studies presented here demonstrate the presence, by the newly developed methods of
260 energy-dependent ALS-active assembly modulator drug resin affinity chromatography and
261 photocrosslinking, of a multi-protein complex in PBMCs that is related to the multi-protein
262 complex observed by the same method in mouse brain and PDFs. As for the drug target in
263 patient-derived fibroblasts (PDFs) where TDP-43 mislocalization and stress-induced aggregation
264 is observed, and also for the target in mouse brain, the drug target in PBMCs has PDI as the
265 direct drug-binding protein. The complex present in human PBMCs also shares with the target in
266 mouse brain and PDFs the presence of RanGTPase, TDP-43, and other proteins, many of which
267 are implicated in the ALS interactome (Figure 2). The precise role of this multi-protein complex
268 drug target in ALS pathophysiology remains to be determined, but based on the efficacy of
269 three structurally unrelated assembly modulators in various animal models, we hypothesize that
270 the drug target serves a role in maintenance of homeostasis. The presence of p62 and
271 optineurin in the complex in PBMCs from healthy individuals, and its loss in ALS patient PBMCs,
272 exacerbated with disease progression (Figure 5), are consistent with this hypothesis.

273

274 Likewise, the appearance of a 17kDa post-translationally modified form of RanGTPase in the
275 drug target isolated from ALS patient PBMCs (Figure 3) suggests a complex biology connected to
276 TDP-43 mislocalization in view of the role of RanGTPase in nucleo-cytoplasmic transport.
277 Moreover, these changes appear very early in ALS, detected in one case so analyzed, prior to
278 onset of severe disability (Figure 4). In all three cases assessed, at a second later time point
279 correlated to disease progression, both of these changes, namely loss of p62 and presence of

280 17kDa PTM RanGTPase, were exacerbated. Taken together with MMP9, which is also enriched
281 in ALS patient PBMC eDRAC bound material, the three signatures identified had a sensitivity of
282 95% and a specificity of 100% for distinguishing ALS patients from healthy individuals. Of course,
283 larger numbers of cases will need to be assessed, but this early degree of discrimination, using
284 as an affinity ligand a drug shown therapeutically active in animal models, is promising as a
285 novel path to an ALS biomarker highly relevant to ALS therapeutics.
286
287 This target multi-protein complex is relevant to ALS for three reasons. First, the drug that served
288 as the ligand to bind and isolate the target is therapeutic in a wide range of ALS cellular and
289 animal models[10]. Second, the composition of the target multi-protein complex includes a
290 number of proteins of the ALS interactome. Third, the isolated target from ALS patient PBMCs is
291 altered in protein composition compared to that from healthy controls. Finally, separate from
292 the specific target in PBMCs a profound degradation of RanGTPase is observed in whole blood
293 from ALS patients but not healthy controls and is rescued upon 72hrs of treatment with ALS-
294 active assembly modulators.
295
296 We interpret these findings to suggest that ALS is, fundamentally, a disease of disrupted
297 homeostasis for which assembly modulators may be therapeutic. Just as the vast majority of
298 individuals don't have cancer for most of their lives, but a small number will develop cancer due
299 to failure of host defenses, so also host defenses protect most of us most of the time from the
300 consequences of various central nervous system insults. A portion of that host defense includes
301 restoration of homeostasis following resolution of a triggering insult. Sometimes however, those

host defenses appear to be incompletely efficacious. As a result, homeostasis is not restored and more and more severe backup mechanisms are engaged in a futile attempt to restore homeostasis. By analogy, when the operating system of your computer is frozen (with appearance of the “colored wheel of doom”), simply attempting to undo the key stroke that caused it will not be effective. Instead, it is necessary to reboot the operating system. Autophagy, in part mediated by p62/SQSTM1 and OPTN, are examples of such a reboot of the operating system for cells and organisms. But what happens when the reboot fails, e.g. due to loss of p62 from the dysfunctional target? We propose the consequence, in a range specific circumstances, is ALS. The persistent deviation from homeostasis is a stress to which motor neurons appear highly sensitive, and eventually, succumb. Once motor neurons have died, the disorder can be stabilized, but no longer fully reversed by restoring homeostasis. Hence the importance of early detection to enable early treatment, which the PBMC signatures noted may provide.

The results of the whole blood experiments (Figure 6) are consistent with the hypothesis that the degradation of whole blood RanGTPase observed, is an extreme feedback response to the inability to restore the target complex back to the healthy state, where elevated RanGTPase and loss of p62 in the eDRAC eluate defined target are signatures of the dysfunctional state. Failure of more proximal feedback loops to correct that dysfunction are hypothesized to trigger a global degradation of RanGTPase in an extreme measure trying, unsuccessfully, to restore homeostasis. Treatment with either of two structurally unrelated assembly modulators results in correction of the RanGTPase degradation observed in whole blood, to a significant extent.

324 This suggests that a multi-step pathway with more than one potential target is involved. We
325 hypothesize that treatment for a longer period would have completely restored RanGTPase
326 levels to normal. Whether assembly modulator drug treatment serves to fully reboot the
327 system, e.g. restore p62, remains to be determined and may vary on a case-by-case basis.
328 Likewise, further studies are needed to determine whether periodic or ongoing drug treatment
329 may be required. Regardless, drug-induced changes in target composition appear to result in
330 restoration of homeostasis at least with respect to RanGTPase degradation. Whether this is
331 reflective of concomitant changes in motor neurons that prevent further motor neuron loss
332 remains to be investigated.
333
334 Our findings are significant for a number of reasons. First, these studies provide a novel window
335 into regulatory feedback loops involved in cellular homeostasis. The precise relationship of the
336 target multi-protein complex in healthy individuals vs ALS patients remains to be more fully
337 understood. One hypothesis is that the target multi-protein complex in healthy individuals is the
338 "normal" assembly machine involved in integration of diverse events of homeostasis. This
339 includes TDP-43 localization, in which RanGTPase likely plays a critical role, perhaps along with
340 C9orf72 and other ALS-implicated gene products. Other relevant pathways including autophagic
341 removal of dysfunctional multi-protein complexes are naturally integrated into the physiological
342 feedback pathways that collectively bring about homeostasis. ALS may be an example where a
343 "stuck" pathway triggers more and more desperate feedback attempts to reboot the system
344 without success, culminating in the mass degradation of RanGTPase observed in the whole
345 blood experiment shown in Figure 5. In this model, the assembly modulator compounds serve

346 to reboot the cellular operating system. A future prediction to be tested, is that longer-term
347 treatment of blood results in complete normalization of RanGTPase – and restoration of
348 p62/SQSTM1 to the target complex present in PBMCs. By virtue of having therapeutic small
349 molecules in hand, the pathways discovered are likely to be productively illuminated by e.g.
350 including by fractionation and reconstitution of functional activities in extracts.
351
352 Second, these data, together with the studies shown previously, suggest that, despite the
353 heterogeneity of ALS presentation and progression, a common underlying pathway is the source
354 of the disease – and that assembly modulators are therapeutic at the underlying shared level.
355 While we hypothesize that restoration of autophagy is a crucial part of this pathway, re-
356 establishment of homeostasis likely involves far more than just restoration of autophagy. In this
357 regards the involvement of miniscule subsets of the specific gene products found together in
358 the target multi-protein complex is notable. These targets could not have been detected by
359 powerful molecular biological tools such as CRISPR or siRNA knockdown studies, because of the
360 heterogeneous roles of small subsets of many, if not most, proteins. Thus the concept of protein
361 "moonlighting" may be more pervasive than is currently generally recognized, and a level of
362 organization of gene expression accessed by protein assembly modulation may be therapeutic
363 for diverse diseases in ways not generally appreciated today.
364
365 Finally, it should be noted that many if not most patients come to medical attention long after
366 the most effective period of treatment is lost. Drugs to stop the disease process may still be
367 effective, but rely on maintenance of the underlying framework of feedback loops to restore

368 homeostasis, once disease progression is arrested. Sometimes however, those feedback loops
369 fail and homeostasis is not restored, whether or not the primary disease process has been
370 blocked. We hypothesize ALS is one such example, making it extremely difficult to treat. The
371 methods described here provide a means of detecting ALS early, prior to onset of severe
372 disability, when it is most treatable – and provide a potentially effective treatment in the form
373 of the small molecule ligands themselves. It is notable that pt 78 came to medical attention
374 early in her clinical course, prior to serious disability, and yet, the signature changes (lowered
375 p62 and elevated RanGTPase 17kDa fragment) were observed, and sadly, progressed
376 culminating in her death. To date, these findings have been observed in over a dozen ALS
377 patients and are lacking in six of six healthy controls. If extended and demonstrated to be ALS-
378 specific, they could enable rapid treatment. That PBMCs are a readily accessible tissue enables
379 early diagnosis prior to motor neuron death, essential for optimal treatment of ALS.
380

381 **Methods**

382 **Preparation of PBMC extracts**

383 Whole blood collected in purple-top EDTA tubes from healthy individuals or ALS patients was
384 shipped by overnight courier to the lab where it was diluted 1:1 with phosphate-buffered saline
385 and layered on ficoll and centrifuged for 15 minutes at 3000 rpm at room temperature. PBMCs
386 were collected at the interface, diluted with PBS 1:1 and centrifuged at 1000 rpm/15 minutes.
387 The supernatant was aspirated and the pellet dissolved in p-body buffer (PBB) consisting of
388 10mM Tris pH 7.5 ,10mM NaCl, 6mM MgAc, 1mM EDTA, and 0.35% Triton-X-100 and
389 centrifuged at 4oC 10,000xg/10min.

390 **Drug Resin affinity chromatography**

391 Mouse brains from wildtype or SOD1 mutant animals were homogenized in cold phosphate
392 buffered saline (PBS) (10mM sodium phosphate, 150 mM sodium chloride pH 7.4), then spun at
393 1,000 rpm for 10 minutes until pelleted. The PBS was decanted and the pellet resuspended in a
394 low salt buffer (10mM HEPES pH 7.6, 10mM NaCl, 1mM MgAc with 0.35% Tritonx100) then
395 centrifuged at 10,000 rpm for 10 minutes at 4°C. The post-mitochondrial supernatant was
396 removed and adjusted to a concentration of approximately 10 mg/ml and equilibrated in a
397 physiologic column buffer (50 mM Hepes ph 7.6, 100 mM KAc, 6 mM MgAc, 1 mM EDTA, 4mM
398 TGA). In some conditions, the extract was supplemented with an energy cocktail (to a final
399 concentration of 1mM rATP, 1mM rGTP, 1mM rCTP, 1mM rUTP, and 5 ug/mL creatine kinase). 30
400 ul or 230 ul of extract was then incubated for one hour at either 4° C or 22° C degrees on 30 ul
401 of affigel resin coupled to THIQ compound or a 4% agarose matrix (control). The input material
402 was collected and the resin was then washed with 3 ml column buffer. The resins were eluted
403 for 2 hours then overnight at 22°C then 4°C in 100ul column buffer containing 100uM of the
404 cognate compound. Eluates were run on western blot or sent for mass spectrometry for
405 analysis.

406

407 **Chemical photocrosslinking**

408 Extract from mouse brain and PDFs grown in minimum essential media were prepared as above
409 then adjusted to a protein concentration of approximately 3 mg/ml in column buffer containing
410 0.01% triton. 1% DMSO or 100uM PAV-073 was added to 6ul of extract, then 3uM of PAV-073
411 photocrosslinker or a negative control crosslinker (comprising of the biotin and diazirine

412 moieties without compound) were added. The extract was incubated for 20 minutes then
413 exposed to UV at 365nM wavelength for 10 minutes then left on ice for one hour. After
414 crosslinking, samples were divided in two 20 ul aliquots and one set was denatured by adding
415 20 uL of column buffer 4ul of 10% SDS, 0.5 ul 1M dithiothreitol (DTT), and heating to 100°C for 5
416 minutes. Both native and denatured aliquots were then diluted in 800 ul column buffer
417 containing 0.1% triton. 5 ul of magnetic streptavidin beads (Pierce) were added to all samples
418 and mixed for one hour at room temperature to capture all biotinylated proteins and co-
419 associated proteins. Samples were placed on a magnetic rack to hold the beads in placed and
420 washed three times with 800 ul of column buffer containing 0.1% triton. After washing, beads
421 were resuspended in 80 ul of gel loading buffer containing SDS and analyzed by western blot or
422 blot for affinity purified streptavidin. Samples were analyzed by western blot.
423
424 **Western blotting**
425 SDS-PAGE gels were transferred in Towbin buffer (25mM Tris, 192mM glycine, 20% w/v
426 methanol) to polyvinylidene fluoride membrane, blocked in 1% bovine serum albumin (BSA) in
427 PBS, incubated overnight at 4°C in a 1:1,000 dilution of 100ug/mL affinity-purified primary IGG
428 to PDI in 1% BSA in PBS containing 0.1% Tween-20 (PBST). Membranes were then washed twice
429 in PBST and incubated for two hours at room temperature in a 1:5000 dilution of secondary
430 anti-rabbit or anti-mouse antibody coupled to alkaline phosphatase in PBST. Membranes were
431 washed two more times in PBST then incubated in a developer solution prepared from 100 uL of
432 7.5 mg/mL 5-bromo-4-chloro-3-indolyl phosphate dissolved in 60% dimethyl formamide (DMF)
433 in water and 100ul of 15 mg/ml nitro blue tetrazolium dissolved in 70% DMF in water, adjusted

434 to 50mL with 0.1 Tris (pH 9.5) and 0.1 mM magnesium chloride. Membranes were scanned and
435 the integrated density of protein band was measured on ImageJ. Averages and the standard
436 deviation between repeated experiments were calculated and plotted on Microsoft Excel.
437
438 **Tandem mass spectrometry**
439 Samples were processed by SDS PAGE using a 10% Bis-tris NuPAGE gel with the 2-(N-
440 morpholino)ethanesulfonic acid buffer system. The mobility region was excised and washed
441 with 25 mM ammonium bicarbonate followed by 15mM acetonitrile. Samples were reduced
442 with 10 mM dithoithreitol and 60° C followed by alkylation with 5o mM iodoacetamide at room
443 temperature. Samples were then digested with trypsin (Promega) overnight (18 hours) at 37° C
444 then quenched with formic acid and desalted using an Empore SD plate. Half of each digested
445 sample was analyzed by LC-MS/MS with a Waters NanoAcquity HPLC system interfaced to a
446 ThermoFisher Q Exactive. Peptides were loaded on a trapping column and eluted over a 75 uM
447 analytical column at 350 nL/min packed with Luna C18 resin (Phenomenex). The mass
448 spectrometer was operated in a data dependent mode, with the Oribtrap operating at 60,000
449 FWHM and 15,000 FWHM for MS and MS/MS respectively. The fifteen most abundant ions
450 were selected for MS/MS.
451
452 Data was searched using a local copy of Mascot (Matrix Science) with the following parameters:
453 Enzyme: Trypsin/P; Database: SwissProt Human (conducted forward and reverse plus common
454 contaminants); Fixed modification: Carbamidomethyl (C) Variable modifications: Oxidation (M),
455 Acetyl (N-term), Pyro-Glu (N-term Q), Deamidation (N/Q) Mass values: Monoisotopic; Peptide

456 Mass Tolerance: 10 ppm; Fragment Mass Tolerance: 0.02 Da; Max Missed Cleavages: 2. The data
457 was analyzed by spectral count methods.
458
459 **Whole blood incubation and analysis**. 100ul aliquots of EDTA-anticoagulated whole blood is dispensed
460 into 24 well plates containing 100ul of room temperature 80% PBS with 10mM glucose and then treated
461 with DMSO to 0.01% or drug in DMSO to the same dilution with final concentration of 5uM drug. After
462 72hrs samples are collected and aliquot 10ul into 1XLB as start material and aliquot another 10ul into
463 1%SDS ECT(1mM rNTPs with 0.2ug/ml CK, 50mM Hepes pH 7.6 100mK KAc, 6mM MgAc and 4mM TGA)
464 at total volume 100ul and incubate at 37°C for 1hr, then put samples into LB. Compared by SDS-PAGE
465 and WB for RanGTPase with whole blood aliquot taken as start material.
466
467 **References**

468 1. Al-Chalabi, A. & Hardiman, O. The epidemiology of ALS: a conspiracy of genes, environment
469 and time. *Nat. Rev. Neurol.* **9**, 617–628 (2013).
470 2. Chiò, A. *et al.* Prognostic factors in ALS: A critical review. *Amyotroph. Lateral Scler. Off. Publ.*
471 *World Fed. Neurol. Res. Group Mot. Neuron Dis.* **10**, 310–323 (2009).
472 3. Gandhi, J. *et al.* Protein misfolding and aggregation in neurodegenerative diseases: a review
473 of pathogeneses, novel detection strategies, and potential therapeutics. *Rev. Neurosci.* **30**,
474 339–358 (2019).
475 4. Grad, L. I., Rouleau, G. A., Ravits, J. & Cashman, N. R. Clinical Spectrum of Amyotrophic
476 Lateral Sclerosis (ALS). *Cold Spring Harb. Perspect. Med.* **7**, (2017).
477 5. Chou, C.-C. *et al.* TDP-43 pathology disrupts nuclear pore complexes and nucleocytoplasmic
478 transport in ALS/FTD. *Nat. Neurosci.* **21**, 228–239 (2018).

479 6. Baradaran-Heravi, Y., Van Broeckhoven, C. & van der Zee, J. Stress granule mediated protein
480 aggregation and underlying gene defects in the FTD-ALS spectrum. *Neurobiol. Dis.* **134**,
481 104639 (2020).
482 7. Gasset-Rosa, F. *et al.* Cytoplasmic TDP-43 De-mixing Independent of Stress Granules Drives
483 Inhibition of Nuclear Import, Loss of Nuclear TDP-43, and Cell Death. *Neuron* **102**, 339-
484 357.e7 (2019).
485 8. Aggad, D., Vérièpe, J., Tauffenberger, A. & Parker, J. A. TDP-43 toxicity proceeds via calcium
486 dysregulation and necrosis in aging Caenorhabditis elegans motor neurons. *J. Neurosci. Off.*
487 *J. Soc. Neurosci.* **34**, 12093–12103 (2014).
488 9. Buratti, E. & Baralle, F. E. Multiple roles of TDP-43 in gene expression, splicing regulation,
489 and human disease. *Front. Biosci. J. Virtual Libr.* **13**, 867–878 (2008).
490 10. Feng Yu, S. *et al. Protein Assembly Modulation: A New Approach to ALS Therapeutics*.
491 http://biorxiv.org/lookup/doi/10.1101/2023.07.24.550252 (2023)
492 doi:10.1101/2023.07.24.550252.
493 11. Marty, L. *et al.* The NADPH-dependent thioredoxin system constitutes a functional backup
494 for cytosolic glutathione reductase in Arabidopsis. *Proc. Natl. Acad. Sci. U. S. A.* **106**, 9109–
495 9114 (2009).
496 12. Noble, D. From Genes to Whole Organs: Connecting Biochemistry to Physiology. in *Novartis*
497 *Foundation Symposia* (eds. Bock, G. R. & Goode, J. A.) vol. 239 111–128 (Wiley, 2001).
498 13. Tomkins, G. M. The metabolic code. *Science* **189**, 760–763 (1975).
499 14. Pardee, A. B. Regulatory Molecular Biology. *Cell Cycle* **5**, 846–852 (2006).

500 15. Pardee, A. B. & Reddy, G. P.-V. Beginnings of feedback inhibition, allostery, and multi-protein
501 complexes. *Gene* **321**, 17–23 (2003).
502 16. Fenton, A. W. Allostery: an illustrated definition for the 'second secret of life'. *Trends*
503 *Biochem. Sci.* **33**, 420–425 (2008).
504 17. Müller-Schiffmann, A. *et al. A Pan-Respiratory Antiviral Chemotype Targeting a Transient*
505 *Host Multiprotein Complex*. http://biorxiv.org/lookup/doi/10.1101/2021.01.17.426875
506 (2021) doi:10.1101/2021.01.17.426875.
507 18. Lingappa, A. F. *et al.* Small Molecule Assembly Modulators with Pan-Cancer Therapeutic
508 Efficacy. *bioRxiv* 2022.09.28.509937 (2022) doi:10.1101/2022.09.28.509937.
509 19. Nardo, G. *et al.* Amyotrophic lateral sclerosis multiprotein biomarkers in peripheral blood
510 mononuclear cells. *PloS One* **6**, e25545 (2011).
511 20. Luotti, S. *et al.* Diagnostic and prognostic values of PBMC proteins in amyotrophic lateral
512 sclerosis. *Neurobiol. Dis.* **139**, 104815 (2020).
513 21. Dervishi, I. *et al.* Protein-protein interactions reveal key canonical pathways, upstream
514 regulators, interactome domains, and novel targets in ALS. *Sci. Rep.* **8**, 14732 (2018).
515 22. Kanehisa, M., Furumichi, M., Sato, Y., Kawashima, M. & Ishiguro-Watanabe, M. KEGG for
516 taxonomy-based analysis of pathways and genomes. *Nucleic Acids Res.* **51**, D587–D592
517 (2023).
518
519
520
521

Supplemental Figure 1

	WT mouse THIQ eluate	WT mouse Control eluate	SOD mouse THIQ eluate	SOD mouse control eluate	healthy PBMC 44 THIQ eluate	healthy PBMC 52 THIQ eluate	ALS PBMC 43 THIQ eluate	ALS PBMC 53 THIQ eluate	ALS PBMC 43 Control eluate	Present in Mouse brain	Present in PBMC	Present in both
ACTN4	2	0	4	0	14	10	28	10	0			
ALDH1A1	2	0	7	0	8	0	0	2	0			
ATP1A1	22	0	17	0	2	5	5	6	0			
ATP2A2	13	0	7	0	2	0	5	0	0			
CALM3	11	0	10	0	13	12	11	12	0			
CCT2	8	0	13	0	7	0	4	0	0			
CCT3	6	0	2	0	8	2	6	2	0			
CCT4	3	0	6	0	8	0	3	2	0			
CCT5	8	0	8	0	9	2	4	0	0			
CCT7	4	0	6	0	8	0	4	2	0			
CCT8	8	0	7	0	11	0	2	2	0			
GSS1G	8	2	10	0	4	4	5	2	0			
GSPS1AA1	27	0	44	0	20	13	11	11	0			
GSPS1AB1	39	0	66	0	28	15	32	8	0			
HSPA2	11	0	15	0	2	7	5	6	0			
HSPB1	4	0	6	0	4	17	13	9	0			
HSPD1	28	2	38	0	17	21	12	9	0			
LDHB	7	0	0	0	14	0	12	0	0			
PKM2	16	0	23	0	14	48	64	43	0			
PRDX1	8	0	11	0	8	6	4	4	0			
PRDX2	7	0	10	0	14	6	9	19	0			
STI1	6	0	11	0	3	0	4	5	0			
STIP1	22	0	21	0	3	8	0	0	0			
TGF1	6	0	5	0	5	0	2	0	0			
TUBA1A	17	0	15	0	10	12	11	18	0			
TUBA4A	16	2	12	0	11	14	14	19	0			
UGP2	12	0	22	0	5	0	7	3	0			
VIM	9	0	35	0	4	0	10	5	0			
YCP	47	2	53	0	15	62	18	15	0			
YWHAB	9	0	0	0	12	6	7	3	0			
YWHAE	9	0	11	0	5	6	6	0	0			
YWHAH	6	0	7	0	4	7	8	0	0			
YWHAQ	10	0	9	0	0	5	6	7	0			
Acln	7	0	3	0	3	0	0	0	0			
Acta1	22	0	0	0	0	0	0	0	0			
Aldh1	6	0	6	0	0	0	0	0	0			
Atca1	3	0	6	0	0	0	0	0	0			
Atp1a1	22	0	14	0	0	0	0	0	0			
Atp1b1	22	0	21	0	0	0	0	0	0			
Atp1a3	20	0	10	0	0	0	0	0	0			
Atp2b1	5	0	6	0	0	0	0	0	0			
Atp2b2	2	0	6	0	0	0	0	0	0			
Atp2b3	20	0	24	0	0	0	0	0	0			
Atp5c1	5	0	6	0	0	0	0	0	0			
Atp5h	5	0	5	0	0	0	0	0	0			
Atp6v1b2	6	0	5	0	0	0	0	0	0			
Atp6v1g2	6	0	8	0	0	0	0	0	0			
Capn2	5	0	2	0	0	0	0	0	0			
Cat	0	0	5	0	0	0	0	0	0			
Ccs	17	0	15	0	0	0	0	0	0			
Cox4i1	7	0	8	0	0	0	0	0	0			
Cox6a1	7	0	11	0	0	0	0	0	0			
Cox6b1	0	0	5	0	0	0	0	0	0			
Ccs	5	0	9	0	0	0	0	0	0			
Dpysl2	11	0	17	2	0	0	0	0	0			
Dynll2	9	0	8	0	0	0	0	0	0			
Eef1b	6	0	6	0	0	0	0	0	0			
Eef1d	5	0	6	0	0	0	0	0	0			
Eif4h1l1	5	0	6	0	0	0	0	0	0			
Epb41l1	5	0	7	0	0	0	0	0	0			
Epn2	5	0	4	0	0	0	0	0	0			
Fasn	14	0	11	0	0	0	0	0	0			
Gapdh	23	3	29	0	0	0	0	0	0			
Gnb	12	0	15	0	0	0	0	0	0			
Gnai1	32	0	40	0	0	0	0	0	0			
Hbb-b1	11	0	11	2	0	0	0	0	0			
Hspa8	14	0	16	0	0	0	0	0	0			
Kif5a	2	0	5	0	0	0	0	0	0			
Lsm6	5	0	4	0	0	0	0	0	0			
Mea1a	19	0	17	0	0	0	0	0	0			
Map1b	7	0	10	0	0	0	0	0	0			
Map6	8	0	9	0	0	0	0	0	0			
Mug1	10	0	10	0	0	0	0	0	0			
Marcks	11	3	7	0	0	0	0	0	0			
Nadk2	2	0	5	0	0	0	0	0	0			
Napa	4	0	6	0	0	0	0	0	0			
Napb	6	0	8	0	0	0	0	0	0			
Nme2	5	0	4	0	0	0	0	0	0			
Nsf1c2	4	0	6	0	0	0	0	0	0			
Nsf2	4	0	8	0	0	0	0	0	0			
Nsf3	0	0	6	0	0	0	0	0	0			
Nsf6	5	0	4	0	0	0	0	0	0			
Nsf	7	0	4	0	0	0	0	0	0			
Nucb1	10	0	11	0	0	0	0	0	0			
Opa1	6	0	5	0	0	0	0	0	0			
Pc	14	0	15	0	0	0	0	0	0			
Pcca1a	14	0	15	0	0	0	0	0	0			
Pdha1	7	0	7	0	0	0	0	0	0			
Pdhb	6	0	6	0	0	0	0	0	0			
Pfkp1	10	0	18	0	0	0	0	0	0			
Pgd	4	0	5	0	0	0	0	0	0			
Pgp1r14	9	0	12	0	0	0	0	0	0			
Pgam1	19	0	31	0	0	0	0	0	0			
Pgp1r10	11	0	0	0	0	0	0	0	0			
Prkaca	5	0	3	0	0	0	0	0	0			
Psma3	5	0	6	0	0	0	0	0	0			
Pygb	36	0	46	0	0	0	0	0	0			
Pygm	26	0	34	0	0	0	0	0	0			
Rpb2	7	0	4	0	0	0	0	0	0			
Scg2	12	0	16	0	0	0	0	0	0			
Slc1a3	3	0	6	0	0	0	0	0	0			
Snc2	7	0	9	0	0	0	0	0	0			
Stx1a3	4	0	5	0	0	0	0	0	0			
Syn9	4	0	5	0	0	0	0	0	0			
Sptan1	31	0	40	0	0	0	0	0	0			
Ssn1b	7	0	10	0	0	0	0	0	0			
Stx6p1	23	0	30	3	0	0	0	0	0			
Syt2	7	0	7	0	0	0	0	0	0			
Tjp1	4	0	6	0	0	0	0	0	0			
Tubb2a	22	0	20	0	0	0	0	0	0			
Tubb3	21	0	18	0	0	0	0	0	0			
Tubb4a	18	0	19	0	0	0	0	0	0			
Tubb5b	22	2	22	0	0	0	0	0	0			
Uae1	6	0	7	0	0	0	0	0	0			
Usp14	3	0	5	0	0	0	0	0	0			
Wac	5	0	4	0	0	0	0	0	0			
ACTN1	0	0	0	0	112	110	111	112	0			
ACTN2	0	0	0	0	0	9	5	6	0			
ANXA1	0	0	0	0	0	2	2	3	0			
ANXA6	0	0	0	0	10	9	7	6	0			
APOA	0	0	0	0	10	7	3	10	0			
APOB48	0	0	0	0	2	0	4	0	0			
ARFC1A	0	0	0	0	5	0	7	3	0			
B2M	0	0	0	0	5	0	4	0	0			
CABP	0	0	0	0	3	0	6	0	0			
CAPN1	0	0	0	0	9	9	11	11	0			
CAPN2	0	0	0	0	6	4	5	4	0			
CAVN1	0	0	0	0	5	6	2	3	2			
CCT6A	0	0	0	0	8	0	4	5	0			
CDC42	0	0	0	0	3	3	5	2	0			
CFL1	0	0	0	0	5	0	3	3	2			
CNDP2	0	0	0	0	11	3	5	5	0			
CORO1A	0	0	0	0	4	7	1	2	0			
COROA	0	0	0	0	0	17	14	10	0			
DJHM1	0	0	0	0	0	0	1	0	0			
EEF1A1	0	0	0	0	11	11	14	6	2			
EHD2	0	0	0	0	0	6	2	2	0			
FLNA	0	0	0	0	12	27	20	26	0			
FBN1P2	0	0	0	0	4	5	19	5	0			
FLNB	0	0	0	0	171	120	149	137	0			
FUBP1	0	0	0	0	8	0	4	0	0			
GAPD	0	0	0	0	4	0	3	4	0			
GC4	0	0	0	0	5	0	3	2	0			
GNAI2	0	0	0	0	6	6	7	5	0			
GDI2	0	0	0	0	17	3	11	7	0			
H3B2	0	0	0	0	24	0	21	24	0			
HBB2	0	0	0	0	4	0	2	8	0			
HIST1H1C	0	0	0	0	0	15	19	0	0			
HIST1H4A	0	0	0	0	5	5	4	6	2			
IQE2	0	0	0	0	5	0	3	8	0			
MRPL23	0	0	0	0	9	0	2	0	0			
MRPS18	0	0	0	0	3	0	6	0	0			
HSPB8L	0	0	0	0	0	4	3	2	0			
HSPA1A	0	0	0	0	3	0	1	0	0			
HSPA8	0	0	0	0	23	22	12	7	2			
H4	0	0	0	0	7	13	21	2	0			
ITGA2B	0	0	0	0	0	2	3	5	0			
ITGB3	0	0	0	0	2	2	3	3	0			
KPNB1	0	0	0	0	5	0	3	0	0			
LCP1	0	0	0	0	10	18	24	8	0			
LDHA	0	0	0	0	11	0	14	6	0			
LTA4H	0	0	0	0	2	0	12	0	0			
LTBP1	0	0	0	0	0	5	2	0	0			
MAPK14	0	0	0	0	6	0	3	4	0			
MMP2	0	0	0	0	0	7	7	6	0			
MPO	0	0	0	0	9	7	17	10	2			
MYH9	0	0	0	0	7	28	12	11	0			
MYL6	0	0	0	0	4	3	7	4	0			
NANP	0	0	0	0	11	0	11	4	0			
NDS1	0	0	0	0	2	23	10	8	0			
PARP1	0	0	0	0	3	5	3	3	0			
PDIA3	0	0	0	0	3	10	7	5	0			
PDLIM5	0	0	0	0	4	13	11	2	2			
PFN1	0	0	0	0	2	6	3	4	0			
PKM	0	0	0	0	0	7	3	0	0			
PPIB	0	0	0	0	3	0	2	8	0			
PGTA	0	0	0	0	18	0	2	6	0			
PRDX6	0	0	0	0	0	6	0	2	0			
PSMC1	0	0	0	0	5	0	2	0	0			
PVR	0	0	0	0	4	0	2	6	0			
RAC2	0	0	0	0	8	6	10	6	0			
RAP1B	0	0	0	0	12	18	15	16	0			
RPL26	0	0	0	0	0	3	3	8	0			
S100A8	0	0	0	0	3	0	7	8	2			
S100A9	0	0	0	0	13	0	13	15	2			
SAMD9	0	0	0	0	15	5	3	0	0			
SELP	0	0	0	0	6	16	6	3	0			
SDPT	0	0	0	0	5	0	4	0	2			
SNCA	0	0	0	0	9	3	5	0	0			
STAT1B	0	0	0	0	7	3	2	0	0			
TMED1	0	0	0	0	21	40	22	22	0			
TCN1	0	0	0	0	61	118	86	56	0			
TPD52L2	0	0	0	0	6	9	6	2	0			
TPM4	0	0	0	0	8	11	4	2	0			
TUBB	0	0	0	0	7	6	13	6	0			
TUBB1	0	0	0	0	3	11	3	3	0			
UBA7	0	0	0	0	8	9	3	0	0			
VGCN	0	0	0	0	0	8	2	2	0			
VCL	0	0	0	0	19	31	24	22	0			
YWHAG	0	0	0	0	7	8	2	6	0			
YWHAZ	0	0	0	0	14	18	15	14	0			
ZYX	0	0	0	0	10	6	14	5	2			

Legend to Supplemental Figure 1. Spectral counts for entire dataset of mouse brain and PBMC THIQ eluates. Colors represent the number of spectral counts for a given protein in each sample, ranging from light green (low counts) to dark green (high counts). The right panel indicates whether a given protein was in one of both of the datasets, according to threshold values of >4 spectral counts in the drug eluate and <4 spectral counts in the control column eluate.

524 **Abbreviations**

525 ALS – Amyotrophic Lateral Sclerosis

526 CFPSA – Cell-free protein synthesis and assembly

527 CNS – Central Nervous System

528 DTT - dithiothreitol

529 DRAC – drug resin affinity chromatography

530 eDRAC – energy-dependent drug resin affinity chromatography

531 FTD – Fronto-Temporal Dementia

532 IND – investigational new drug

533 MS-MS – tandem mass spectrometry

534 PBMC – Peripheral blood mononuclear cell

535 PDF – patient-derived fibroblast

536 PDI – protein disulfide isomerase

537 PTM – post-translationally modified

538 SAP – streptavidin precipitation

539 SDS-PAGE – polyacrylamide gel electrophoresis in sodium dodecyl sulfate

540 WB – western blot

541

542 **Acknowledgments**

543 We thank Target ALS (grant# IL-2023-C4-L1), DOD CDMRP (grant #. W81XWH2210721), and Prosetta

544 Biosciences for financial support

545

546 **Competing Interests**

547 VRL is CEO of Prosetta Biosciences

548

549

550

551

552

553